

AD-A267 651 INTATION PAGE



Form Approved
OMB No. 0704-0188

1. AGENCY USE ONLY (Leave blank)		2. REPORT DATE 1993	3. REPORT TYPE AND DATES COVERED THESIS/ DISSERTATION																							
4. TITLE AND SUBTITLE Orographic Microbursts in a Severe Winter Windstorm			5. FUNDING NUMBERS																							
6. AUTHOR(S) Zena A. Tucker																										
7. PERFORMING ORGANIZATION NAME(S) AND ADDRESS(ES) AFIT Student Attending: North Carolina State Univ			8. PERFORMING ORGANIZATION REPORT NUMBER AFIT/CI/CIA- 93-019																							
9. SPONSORING/MONITORING AGENCY NAME(S) AND ADDRESS(ES) DEPARTMENT OF THE AIR FORCE AFIT/CI 2950 P STREET WRIGHT-PATTERSON AFB OH 45433-7765			10. SPONSORING/MONITORING AGENCY REPORT NUMBER																							
11. SUPPLEMENTARY NOTES																										
12a. DISTRIBUTION AVAILABILITY STATEMENT Approved for Public Release IAW 190-1 Distribution Unlimited MICHAEL M. BRICKER, SMSgt, USAF Chief Administration			12b. DISTRIBUTION CODE																							
13. ABSTRACT (Maximum 200 words)																										
<table border="1"> <tr> <td colspan="2">Accession For</td> </tr> <tr> <td>NTIS GRA&I</td> <td><input checked="" type="checkbox"/></td> </tr> <tr> <td>DTIC TAB</td> <td><input type="checkbox"/></td> </tr> <tr> <td>Unannounced</td> <td><input type="checkbox"/></td> </tr> <tr> <td>Justification</td> <td></td> </tr> <tr> <td colspan="2">By _____</td> </tr> <tr> <td colspan="2">Distribution/</td> </tr> <tr> <td colspan="2">Availability Codes</td> </tr> <tr> <td colspan="2">Avail and/or</td> </tr> <tr> <td>Dist</td> <td>Special</td> </tr> <tr> <td>A-1</td> <td></td> </tr> </table>					Accession For		NTIS GRA&I	<input checked="" type="checkbox"/>	DTIC TAB	<input type="checkbox"/>	Unannounced	<input type="checkbox"/>	Justification		By _____		Distribution/		Availability Codes		Avail and/or		Dist	Special	A-1	
Accession For																										
NTIS GRA&I	<input checked="" type="checkbox"/>																									
DTIC TAB	<input type="checkbox"/>																									
Unannounced	<input type="checkbox"/>																									
Justification																										
By _____																										
Distribution/																										
Availability Codes																										
Avail and/or																										
Dist	Special																									
A-1																										
14. SUBJECT TERMS DTIC QUALITY INSPECTED 3			15. NUMBER OF PAGES 43																							
			16. PRICE CODE																							
17. SECURITY CLASSIFICATION OF REPORT	18. SECURITY CLASSIFICATION OF THIS PAGE	19. SECURITY CLASSIFICATION OF ABSTRACT	20. LIMITATION OF ABSTRACT																							

DTIC
SELECTED
S B D
AUG 11 1993

93-18517

DISCLAIMER NOTICE



THIS DOCUMENT IS BEST
QUALITY AVAILABLE. THE COPY
FURNISHED TO DTIC CONTAINED
A SIGNIFICANT NUMBER OF
PAGES WHICH DO NOT
REPRODUCE LEGIBLY.

ABSTRACT

TUCKER, ZENA ANN. Orographic Microbursts in a Severe Winter Windstorm.
(under the direction of Steven Businger).

Orographic microbursts in a remarkable winter wind storm caused severe damage to the San Juan Islands and coastal regions of Washington State on December 28, 1990. The microbursts, associated with trapped lee mountain waves, produced winds in excess of 50 m s^{-1} on Guemes Island. The damage patterns of the tree fall and debris reveal small scale swaths and pockets of high winds similar to those patterns caused by convective downbursts.

Analysis of large scale features reveal that an underlying cause of the strong winds was a strong pressure gradient behind an arctic front. The strong pressure gradient was due to cold air damming on the eastern slopes of the Canadian Coast and Cascade Mountains. Gap wind acceleration was noted over Puget Sound by the sharp boundary between the high speed jet of dry air emanating from the Fraser River Valley, a gap between the Coast and Cascade Mountains, and the ambient lower speed marine winds.

However, the synoptic scale pressure gradient and gap winds cannot explain the rapid onset of the destructive gusts of $40\text{-}50 \text{ m s}^{-1}$ and the small scale damage swaths on the San Juan Islands. Downslope amplification from the nearby mountains was the likely cause. Cross-mountain flow, a stable layer at ridge top, and a mid-level critical layer indicate mountain wave amplification. Lee eddies, or orographic microbursts, are generated by severe downslope windstorms and are known to cause considerable damage on small scales. Therefore, it was concluded that the destructive winds over the San Juan Islands were due to the concurrent influences of downslope

amplification, gap wind acceleration and the strong synoptic scale pressure gradient.

OROGRAPHIC MICROBURSTS IN A SEVERE WINTER WINDSTORM

by
ZENA ANN TUCKER

A thesis submitted to the Graduate Faculty of
North Carolina State University
in partial fulfillment of the
requirements for the Degree of
Master of Science

**DEPARTMENT OF MARINE, EARTH AND
ATMOSPHERIC SCIENCES**

Raleigh

1993

APPROVED BY:

Gerald P. Watson *Pinky Stewart*

Elmer C. Sizer, Jr.
Chair of Advisory Committee

BIOGRAPHY

Zena Ann Godsey Tucker was born on March 2, 1961 in Jasper, Alabama. She is a Captain in the U. S. Air Force.

ACKNOWLEDGMENTS

Thanks to the University of Washington, Department of Atmospheric Sciences, the US. Air Force Environmental Technical Assistance Center and the Canadian Environmental Services for the providing data for this study. We thank Bob Banton and Micheal Hardesty at the NOAA Environmental Laboratories in Boulder, Colorado for their helpful conversations and reference material. This material was supported by the NSF Grant ATM-9121126 and COMET Grant UCAR-S9121.

Thanks to Bill Spendley and to Steve Chiswell for help with GEMPAK. Thanks to John Grovenstein, the Macintosh wizard and running partner. I owe special gratitude to my advisory committee, especially Dr. Businger. I especially appreciate the support of the U. S. Air Force, which made my presence here possible. Most of all, thanks to my husband, Rick and my children.

TABLE OF CONTENTS

LIST OF FIGURESv

1. Introduction1

2. Synoptic Overview3

3. Mesoscale Analyses7

4. Development of the Downslope Windstorm10

5. Discussion and Conclusions17

References41

LIST OF FIGURES

Figure 1. Location and topographic map of western Washington and southwest British Columbia.	22
Figure 2. One of the trees toppled by the storm	23
Figure 3. Forest damage on Guemes Island	24
Figure 4. Aerial photo of damage swath on Guemes Island	25
Figure 5(a) Sea level pressure and frontal analysis for 1200 UTC 27 December 1990. Analysis of height for 850 mb(b) and 500 mb(c)	27
Figure 6. Same as figure 5 except for 0000 UTC 28 December 1990.....	28
Figure 7. Same as figure 5 except for 1200 UTC 28 December 1990.....	29
Figure 8. 500 mb height and vorticity analysis valid 1200 UTC 28 December 1990.....	30
Figure 9. Same as figure 5 except for 0000 UTC 29 December 1990.....	31
Figure 10. Regional surface chart for 0600 UTC 28 December 1990.	32
Figure 11. Regional surface chart for 1200 UTC 28 December 1990.	33
Figure 12. Time of arrival at selected stations of the arctic air mass based on dew point (4°C) and wind velocity (10 m s^{-1}).	34
Figure 13. Regional surface chart for 1800 UTC 28 December 1990.	35
Figure 14. Comparison of pressure difference between BLI and YYF and average wind speed (a) and gust wind speeds (b) at BLI.	36
Figure 15. Skew T -log p plot: Temperature, dew point and wind vertical profile for Vernon, British Columbia at 1200 UTC 28 December 1990.....	37
Figure 16. Same as figure 15 except for 0000 UTC 29 December 1990.....	38
Figure 17. Cross section of potential temperature along dashed line in figure 5(b).	39

Figure 18. Idealized schematic of the downslope windstorm of 28

December 1990.....40

1. Introduction

During the early morning hours of 28 December 1990, an arctic front blasted northwestern Washington State. For over twelve hours an ensuing windstorm persisted with peak gusts observed at 50 m s^{-1} . The damage from the strong winds extended from the San Juan Islands through the Strait of Georgia and southward through Puget Sound. While strong winds are not unusual for western Washington State, this storm was noteworthy because of the unprecedented damage to the San Juan Islands. Residents believe the hurricane force winds were the most severe experienced this century, an observation supported by the character of the forest damage.

Prior to the arrival of the windstorm, temperatures were near normal, with southwesterly winds, overcast skies and occasional periods of light rain or snow. The arctic front moved swiftly from the northeast, heralding an extremely dry continental polar air mass. Winds shifted from the southwest to the northeast and grew stronger with each passing hour. Winds were strong with gusts of 20 m s^{-1} until late the next day. Peak gusts of over 25 m s^{-1} occurred near midnight at Bellingham on the coast of Puget Sound at the southern end of the Fraser River Valley.

The combination of high tides and intensely strong and cold northerly winds caused substantial damage along the exposed waterfront areas from Bellingham (BLI) south through Puget Sound (see fig. 1 for location map)

On Fidalgo and Whidbey Islands winds destroyed marinas and houseboats as well as a few homes. Power and telephone service was knocked out for several hours. On Samish and Guemes Islands, oyster and clam beds were wiped out by high tides. Forest damage was widespread in the San Juan Islands with the greatest damage on Sinclair and Guemes Islands. Figure 2 shows one of the

many massive century old trees that were toppled by the winds. Two people were killed and one injured by falling trees. (NOAA Storm Data, 1990).

On Guemes Island a resident described the events of 28 December: At midnight, electric service stopped as high winds broke small tree branches. Large branches were breaking by 2 am. After 3 am, large trees were falling under the force of the intense winds. High winds and destruction of large trees continued until around 8 am when winds eased. However, occasional large gusts toppled weakened trees from 8 am until the afternoon of 28 December.

The forest damage was carefully surveyed by local residents and Dr. Businger. Figure 3 illustrates the damage pattern on Guemes Island. Interestingly, the 30 - 45 m tall trees were felled in swaths about 200 m long and 50 m wide. Outside the swaths, only scattered damage occurred (see aerial photo in figure 4). The individual swaths are oriented in the direction of the prevailing wind. However, the swaths occur in groups of 3 or 4 which are oriented perpendicular to the mean wind. This damage pattern strongly resembles the 1-2 km narrow swaths caused by the severe wind storm in the lee of the Cascades documented by Mass and Albright (1985). This similarity suggests a common mechanism for the narrow bands of straight line winds. We refer to this phenomena as the *orographic microburst*. Like the convective microburst, the damage covers less than 5 km.

This unique characteristic of downslope windstorms has been newly investigated. Pulsations of intensely strong winds have been observed by Doppler lidar in a Boulder, Colorado windstorm (Nieman, et al., 1988). The wind gusts propagate downstream at the speed of the mean flow and cause peak winds at the surface every 8 to 10 minutes. These wind maximums are extremely difficult to observe with a normal observation network and are

responsible for small scale damage patterns in Boulder, Colorado (Bedard, 1990). These pulsations can be discerned by examination of damage patterns similar to the method used by Fujita (1985) in the study of microbursts. The damage documented by Bedard is remarkably similar to that on Guemes Island. Unlike downdrafts studied by Fujita, these microbursts are not due to convection, but are the result of traveling wind pulsations associated with the turbulent region of a lee side hydraulic jump. Thus, a new term is applied to the downslope windstorm pockets of high winds: orographic microbursts.

The physical mechanism producing these pulsations has been identified as Kelvin-Helmholtz (K-H) instability in the lee of the obstacle (Peltier and Scinocca, 1990; Smith, 1991). In their modeling studies these disturbances propagated downstream at a speed slower than the low-level winds and were only found well downstream of an orographic ridge. According to Peltier and Scinocca, the K-H instability on the "shear interface between the low level jet and the upper level decelerated layer" leads to the wind pulsation.

An investigation of the synoptic and mesoscale conditions that led up to the 28 December 1990 storm was undertaken in the hopes of improving our understanding of these destructive winter windstorms. The specific contributions of downslope amplification and gap wind effects are documented in this paper.

2. Synoptic Overview

To examine the large scale interaction that brought on the destructive wind storm, synoptic scale analysis is performed using operational National Weather Service surface observations and upper air soundings over the western United States and Canada. Observations were also obtained from buoys, refineries and bridges throughout the inland waters of Washington State. In

data sparse regions, the initial analysis of the Nested Grid Model (NGM) is used for 27 December 1990 at 1200 UTC.

Prior to the storm, Washington State experienced an unusually cold December. However, temperatures were near normal after Christmas with winds from the southwest along the coast.

On 27 December 1990 at 1200 UTC (Fig. 5a), 24 hours prior to the peak winds, arctic air extended from the Canadian Yukon territories to the US. Canadian border. A cold front stretched through western British Columbia and marked the boundary between the relatively warm marine air mass and the dry arctic air. At 850 mb the trough associated with the front extended from a low in central Canada northwestward (Fig. 5b). The trough became inverted over northwestern British Columbia in a region of strong baroclinicity. Further aloft at 500 mb, a strong short-wave trough stretched from the Northwest Territories to northern British Columbia (Fig. 5c). The trough was amplified over western British Columbia in the baroclinic region. An associated jet streak paralleled western Canada and turned cyclonically eastward over northern Washington. The left entrance region of the jet streak is just east of the surface cold front over northern British Columbia. The direct circulation induced by the jet places the region of strong convergence aloft associated with the left entrance region of the jet directly behind the surface front. Thus, this portion of the front is located in an area of strong large scale subsidence.

Twelve hours later on 28 December at 0000 UTC, the Canadian anticyclone intensified and moved south in response to the strong subsidence aloft (Fig. 6a). The arctic air has passed across central Canada and into northern Montana by this time. However, impeded by the Coast and Rocky Mountains, the cold

front has moved only minimally westward. The pressure gradient across the Coast Range in southeastern British Columbia is strong after the passage of the arctic front. Also noteworthy is the ageostrophic angle between the surface winds and the isobars over British Columbia. The ageostrophic flow east of the Coast and Cascade mountains is associated with cold air damming. The stable dense air from the arctic anticyclone was forced up the barrier and deflected parallel to the mountains in a manner similar to previously studied cases of cold air damming in the Rocky (Dunn, 1987) and Appalachian Mountains (Bell and Bosart, 1988; Richwein, 1980). As a result of the cold air damming a "nose" of high pressure is evident at 850 mb (Fig 6b) just east of the mountains. The cold air damming and the warm moist low level flow from the Pacific Ocean intensified the front over British Columbia in a similar manner to the formation of the Piedmont front over the Carolinas (Businger et al. 1991).

At 500 mb, the short-wave trough has moved southeastward and caused significant height and temperature falls over the Pacific Northwest (Fig. 6c). The jet stream remains parallel to the west coast of Canada, and strongest subsidence associated with the left entrance region remains over west central British Columbia. The windstorm began over western Washington 1-2 hours after the passage of the cold front.

On 28 December at 1200 UTC the winds were at their peak over Guemes Island. The cold front has moved quickly through the region (Fig. 7a). The pressure gradient across the Coast Ranges and the Cascade Mountains remains strong with an 11 mb difference between Vernon, British Columbia (WVK) and Bellingham, WA (BLI). At 850 mb, the inverted trough over the west coast of British Columbia has flattened, due to the strong subsidence aloft and the weakening of the 850 mb low over Washington state (Fig 7b). Consequently,

the geostrophic winds over the Coast Range are from the east, in direct cross-mountain flow at 850 mb (the average mountain height).

At 500 mb the short-wave trough is directly over the Coast and Cascade Mountains(Fig. 7c). With the passage of this short-wave, the 500 mb flow turns rapidly from westerly to northerly. The area of strong convergence aloft associated with the left entrance region of the jet has now moved over southern British Columbia. Significant negative vorticity advection also contributes to the upper convergence (Fig. 8). These synoptic scale processes placed strong downward vertical motion over northwestern Washington state.

The violent boreal winds began in the early morning hours just after midnight local time, and reached their peak around 4 a.m. LST. Strong winds continued until the afternoon on 28 December 1990. By evening peak gusts were below 25 m s^{-1} . Meanwhile, temperatures and dew points plummeted, with BLI reporting a temperature of $-12 \text{ }^{\circ}\text{C}$ at 0000 UTC on 29 December. The surface front moved completely through Washington. The pressure gradient across the mountains weakened slightly to less than 10 mb between BLI and Penticton British Columbia in the Fraser River Valley (Fig. 9a). At 850 mb the inverted trough weakened further, but geostrophic winds over Washington remain cross-mountain (Fig. 9b). Aloft the short-wave trough and the entrance region of the jet streak have moved southeast out of Washington state (Fig. 9c).

From this synoptic scale analysis we see a fundamental cause for the windstorm was the passage of the arctic front and the strong pressure gradient behind it. The very dense air over British Columbia was blocked to the west by the Coast Mountains in a case of cold air damming. Aloft, strong subsidence associated with strong negative vorticity advection and a jet streak

contributed to the exceptionally strong pressure gradient behind the cold front.

3. Mesoscale Analyses

For more detailed regional analysis, additional surface observations were obtained from buoys, bridges and oil refineries in the region. These stations are not standard reporting stations and are denoted by four letter identifiers in figure 12.

At 0600 UTC 28 December, just prior to the windstorm, the arctic front had just passed through the Strait of Georgia and the San Juan Islands (Fig. 10). The pressure and thermal gradient were especially strong behind the front over British Columbia in the region of cold air damming. Funneling of the arctic air through the Fraser River Valley is revealed by the northeasterly winds at Bellingham and other stations in the valley and by the high pressure ridge in the gap between the mountains.

At 1200 UTC 28 December winds gusted over 25 m s^{-1} at Bellingham while less than 50 km to the southwest, winds at Guemes were unofficially clocked to 50 m s^{-1} . Winds in Puget Sound and the Strait of Juan de Fuca at this time are ageostrophic, blowing parallel to the pressure gradient and to the coastline (Fig 11). This localized flow is a manifestation of gap winds. The high bluffs and hills along the shores of the Strait of Georgia and Puget Sound funneled the north northeasterly winds into a relatively narrow dry jet stream.

Reed (1931) first studied how the strength and direction of local winds were influenced by the Straits of Georgia and Juan de Fuca. He defined gap winds as relatively homogeneous air in a sea channel with a source region at one end. In this case the source region is the cold air flowing from the anticyclone in British Columbia through the Fraser River Valley.

Overland and Walter (1981) used instrumented aircraft and a dense network of surface observations to further study gap winds in the region. While gap winds were noted in a variety of synoptic regimes, the anticyclonic event of 13 February 1979 is akin to the case described here. The gap winds are well defined by a distinct dew point gradient and horizontal wind shear. The low level winds were prevented from spreading horizontally not only by the terrain, but by the strong pressure gradient parallel to the channel.

Gap wind effects were traced in the 28 December 1990 case by tracking the time of arrival of the low-dew point (4°C) high-speed (10 m s^{-1}) winds that were typical of the arctic air mass. Figure 12 shows the first stations to measure the outflow in western Washington were west of the Fraser River Valley. The gap winds pushed through Puget Sound aided by the north-south oriented pressure gradient.

By 28 December at 1800 UTC (28/1300L) the destructive northeasterly winds had ceased over the San Juan Islands, but gust wind speeds were still above gale force (18 m s^{-1}). Wind speeds were at their maximum over the Puget Sound where the gap wind effects were most prevalent (Fig. 13)

A graphical depiction of the surface wind speeds on the coast of Puget Sound and sea level pressure gradients for the storm is given in figure 14. The average wind speed (Fig. 14a) and the peak winds (Fig. 14b) at Bellingham show correspondence with the pressure gradient though the mountain gap. In general as the pressure difference between Bellingham (BLI) and Penticton British Columbia (YYF) increased, so did the wind speeds at Bellingham.

To determine if the observed pressure gradient was sufficient to produce the strong winds at Bellingham, we used scaled equation of motion for frictionless flow through a channel (Overland and Walter, 1981):

$$\frac{du}{dt} = \frac{d}{dx} \left(\frac{u^2}{2} \right) = -\frac{1}{\rho} \frac{\partial p}{\partial x}$$

Wind speed is u , p is pressure and ρ is density. For flow at a fixed height this equation can be integrated to yield the Bernoulli equation

$$\frac{u_2^2}{2} = \frac{u_1^2}{2} - \frac{\Delta p}{\rho},$$

where u_1 is the entrance velocity, u_2 is the exit velocity and $\Delta p = p_2 - p_1$, the pressure difference between the exit and entrance points (Reed, 1981).

We can apply this form of the Bernoulli equation since there is a small difference in elevation between BLI and YYF (both in the Fraser River Valley). With a pressure difference of 11 mb observed at 1200 UTC and an entrance speed of 10 m s^{-1} at YYF, the computed speed for Bellingham is 44 m s^{-1} . This wind speed is much larger than the observed maximum gust of 28 m s^{-1} . This discrepancy is likely due to the effects of surface friction. Thus the observed pressure gradient was more than sufficient to account for the high winds at Bellingham.

The strong relationship between the pressure gradient and windspeed is well known for windstorms in the lee of the Cascade Mountains (Reed, 1981; Mass and Albright, 1985) and is operationally used to aid in wind forecasting. In this case, the NGM surface prognosis (not shown) predicted well the development of the strong pressure gradient over British Columbia and western Washington. With the model guidance and knowledge of the fore mentioned relationship successful prediction of a strong windstorm was possible.

Thus far we have determined that the windstorm of 28 December 1990 was caused in part by the strong pressure gradient brought on by cold air

damming behind an arctic cold front. Gap wind effects were also very evident over the Fraser River Valley, Puget Sound, and the Straits of Georgia and Juan de Fuca.

However, channel effects through the mountain gap do not explain the rapid onset of the destructive winds during the early morning hours. Also, gap winds cannot account for the unusual damage pattern found on the San Juan Islands. Since the nearby terrain is mountainous, we must examine the effects of flow *over* the barriers as well. Mountain wave amplification during the storm will explain these phenomenon. The microburst winds were not thunderstorm related, but were due to eddies in accelerated orographic flow

4. Development of the Downslope Windstorm

In this section, a brief review of the fundamental aspects of downslope windstorms is given to determine the conditions favorable for downslope winds. The vertical structure of the upwind storm environment is then explored to assess the possibility of downslope amplification in the case of 28 December 1990.

Three conceptual models attempt to explain the downslope windstorm. The oldest of the models proposed by Long in the early 1950's (Long, 1953) appears to be the most successful (Durrant, 1986, 1990). The theory simply stated: the downslope windstorm is the atmospheric equivalent of shallow water flow over a rock that produces a hydraulic jump on the lee side of the obstacle.

However the atmosphere has no "rigid lid" that prevents vertical energy transport through the hydraulic layer. The vertically propagating wave theories (Klemp and Lilly, 1975; Lilly and Klemp, 1979) proposed that the strong lee side winds were due to partial reflection of the vertically propagating wave induced by the mountain. Partial reflection occurs when

the wave encounters a layer of sharp vertical variation in stability and wind resulting in a trapped lee wave (Scorer, 1949). Maximum downslope winds are achieved when the troposphere is "tuned" such that the upward and downward propagating waves are resonant. The most important tuning requirement was determined observationally (Bower and Durran, 1986) and numerically (Lilly and Klemp, 1975) to be a non dimensional vertical phase shift value of 0.5 or π radians.

The phase shift is given by (Bower and Durran, 1986):

$$\phi = \frac{1}{2\pi} \int_{z_0}^{z_t} l dz$$

where z_t and z_0 are the heights of the tropopause and the top of the stagnant air blocked upstream respectively and l is the Scorer parameter. The Scorer parameter is given by:

$$l^2 = \frac{N^2}{U^2} - \frac{1}{U} \frac{d^2 U}{dz^2}$$

where N is the Brunt-Väisälä frequency (a measure of the static stability) and U is the horizontal wind component normal to the ridge crest. The Scorer parameter corresponds to the vertical wave number in the linear, hydrostatic, steady state equation for vertical velocity. Observational evidence (Bower and Durran, 1986) indicates that this theory has some utility in predicting windstorms in Boulder Colorado.

However, since the phase shift is strongly dependent of the vertical integration of U the theory is limited to cases where there is deep cross-mountain flow. The theory is also limited in practice since calculation of the curvature term of the Scorer parameter is difficult using standard rawinsonde

observations. Therefore the phase shift is calculated using only the first term of the Scorer parameter.

A third explanation also explains how the upward propagating mountain wave energy can be reflected. Numerical investigations by Clark and Peltier (1977, 1984), Peltier and Clark (1979, 1983) and Clark and Farley (1984) revealed that downslope windstorms develop when vertically propagating waves overturn and create a region of localized flow reversal. Smith (1985) and Smith and Sun (1987) created a new mathematical model based on the assumption that the flow reversal layer is an effective upper boundary. Smith's model assumes that the flow above the boundary is relatively undisturbed, while below the dividing streamline the flow transitions from subcritical to supercritical when the critical level is at an ideal height.

All the above theories provide insight into the dynamics of the severe downslope windstorms. The latter two theories provide explanations of how vertically propagating mountain wave energy is reflected downward to produce the severe downslope windstorm. All theories have a communality in that once the severe downslope windstorm is occurring, the flow over the mountain is accelerated first by the pressure gradient at the mountain crest and then by gravity on the lee side as originally described by hydraulic theory.

These theories are diagnostic tools, however, and cannot provide timely forecasts of severe downslope windstorms. Never-the-less, with the knowledge of the typical environment of the windstorms provided by the theories, climatologies were compiled for windstorms in Boulder, Colorado (Brinkmann, 1974; Bower and Durran, 1986), Senj, Yugoslavia (Smith, 1987) and Juneau,

Alaska (Colman and Dierking, 1992) to name a few. Two criteria are common to most of the windstorms and are useful forecasting guides:

- 1) The upstream temperature profile exhibits a shallow ridge-top inversion or layer of strong stability.

- 2) The flow is cross-mountain at ridgetop.

Two additional criteria are also useful to note, but are not sufficient alone to produce the severe wind state:

- 1) Cross-barrier flow decreases with height and eventually reverses in the critical layer. This criteria is useful in wave-breaking regimes.

- 2) In instances when there is no critical layer aloft, a vertical wavelength phase shift of 0.5.

With these criteria in mind, the data from the 28 December 1990 windstorm is examined.

Since the winds during the storm over the San Juan Islands were from the northeast out of the Fraser River Valley, logically the upwind sounding in this case would be upwind in British Columbia and on the upwind side of the mountains. Thus Vernon, British Columbia (WVK) was chosen as representative of the upstream cold continental airmass.

Prior to the windstorm, the 850 mb chart for 28 December at 0000 UTC (Fig. 6b) indicates the flow was not cross-mountain over the Pacific Northwest. The WVK sounding at the same time (not shown) indicates only a weak stable layer below the average mountain height (2000 m). Therefore, downslope amplification was unlikely at this time.

At 1200 UTC on 28 December during the peak winds on Guemes Island, the 850 mb chart (Fig. 7b) shows winds at mountain top are from the northeast (cross-mountain). The upstream sounding (Fig. 15) shows a stable layer

between 790-680 mb (just above the average mountain height). At 620 mb winds rapidly shift, backing from the west. It is likely that this wind shift aloft is present downstream over the mountain since the 500 mb chart (Fig. 7c) shows that winds were most likely from the west northwest as the synoptic scale short wave trough passed. This windshift at mid level in the troposphere is flow reversal and represents a critical level

Since the windstorm environment has a strong windshift away from cross mountain flow or a critical level, this windstorm was not of the resonant reflection class and calculation of the phase shift is not applicable.

In summary, the 1200 UTC data indicates that three of the criteria common in downslope windstorms were present: the upstream stable layer, cross-mountain flow at ridgetop, and an apparent critical layer indicated by the strong wind shift aloft.

However, this windstorm environment is different from typical Boulder, Colorado windstorms. The WVK sounding indicates a thick layer of moist air above the mountain height not common of strong Boulder storms. Since the air that reached the San Juan Islands was warmer (though still cold by local standards) and dry, adiabatic heating must have occurred. The moisture present had the likely effect of suppressing even stronger winds from occurring on the lee side (Durrant and Klemp, 1982).

Also, the stable layer indicated by the WVK sounding is not shallow like the typical 25 mb thick layer observed in Colorado storms (Brinkmann, 1974). However, composite soundings for windstorms in Alaska and cross-sections of windstorms in Yugoslavia indicate stable layers up to 100 mb (1 km) thick. Also, soundings taken upstream during severe windstorms in the lee of the Cascade Mountains have thick stable layers at ridgetop (Reed, 1981; Mass and

Albright, 1985). Thus it appears that stable layer thickness is not crucial to the downslope windstorm environment.

Twelve hours later the destructive 50 m s^{-1} winds had abated. While at the surface, the pressure gradient across the mountains is still strong at 10 mb, the Bellingham wind speeds are markedly lower. The vertical structure of the atmosphere on 29 December at 0000 UTC will explain this decrease in storm intensity. The 850 mb chart (Fig. 8b) shows the flow remained cross-mountain over the Coast Mountains. However the WVK sounding (Fig. 16) indicates the layer above 790 mb (above mountains) is less stable than the previous sounding. Also the marked mid-level wind shift present earlier has vanished. Winds below 500 mb are northeasterly in cross mountain direction.

Since there is no critical layer, calculation of phase shift from the WVK sounding is possible. A phase shift value of 0.67 was calculated between the top of the blocked layer at 2000 m to the tropopause at 6400 m. This value indicates that the atmosphere is not optimally tuned for resonant reflection. Thus, the upstream environment evolved away from the previously observed downslope windstorm criteria. The implication is the winds have ceased to be destructive because the mountain wave amplification environment no longer exists.

A traditional means of visualizing the flow during downslope windstorms is the isentropic cross-section. A cross section of potential temperature for 28 December 1200 UTC was compiled using soundings along the dashed line in figure 7b and surface potential temperatures downstream of the Coast mountains. The cross-section path was chosen roughly along the parcel trajectory. Figure 17 illustrates the isentrope convergence upstream of the mountains, the stable layer above the mountains, and the isentrope descent on the lee side of the mountains.

With this cross-section and other storm data, we can make practical application of Smith's hydraulic theory (Smith, 1985). With values of the height of the critical streamline upstream (H_0), depth between the critical streamline downstream of the mountain and H_0 (δ_c), the upstream wind speed, (U_0) and N , we can calculate the downstream windspeed due to mountain wave acceleration. The idealized schematic of the flow given in figure 18 illustrates these values for this case.

From the cross-section, H_0 is the level of the isentrope upstream of the Coast Mountains that is relatively unaffected by the mountain wave. A reasonable estimate is 700 mb or 3000 m. We cannot accurately determine δ_c without profile data from within the severe winds. However, since the accelerated flow on the lee-side of the mountain is very shallow, we can say $\delta_c \approx H_0$ without causing significant error. From the NGM prognosis for the grid points closest to the mountains, U_0 was determined to be 15 m s^{-1} . N_0 was calculated from the WVK sounding. A value of 0.02 s^{-1} was obtained from the layer between the top of the mountain (2000 m) and the critical layer at 620 mb (3900 m).

The surface horizontal wind equation was adapted from equation 2.17

$$u = U_0(1 + H_0 l \cos H_0 l) \text{ (Smith 1985)}$$

where $l = N_0/U_0$. This equation was used to calculate a downstream windspeed of 75 m s^{-1} . This windspeed compares well with the windspeed of 75 m s^{-1} calculated from the F2 scale damage on San Juan Islands (Fujita, 1985).

Another comparison between theory and observations can be made. Smith's theory predicts that for a given mountain height and upstream environment, the flow will only transition to the severe wind state when $H_0 l$ is at a unique ideal value. By estimation from the cross-section on 28 December 1990, the

airflow is blocked on the eastern side of the Coast Mountains up to about 1500 m. Therefore the *effective* mountain height (h_e) is the actual height minus the depth of the blocked layer, or 500 m. For a value of $h_e l = .66$, then the theoretical ideal value of $H_0 l$ is 3.9. We solve for H_0 to get a theoretical height of the critical streamline of 2925 m. This calculated value compares well with the observed value of 3000 m estimated from the cross-section.

So while Smiths theory cannot predict the occurrence of the severe windstorm, these calculations indicate that the theory does have practical utility to the local forecaster. Once the determination that mountain-wave amplification will occur, then these simple calculations can determine the maximum winds in the orographic microbursts.

5. Discussion and Conclusions

This paper has described the exceptional windstorm that struck northwest Washington State on 28 December 1990. While damage was widespread, the most severe damage was downwind of the Fraser River Valley, a gap between the Cascade and Coast mountains. Winds, clocked as high as 50 m s^{-1} , caused destruction across the San Juan Islands and through Puget Sound.

Prior to the storm, an arctic front passed through the region from the northeast. Behind the front, an exceptionally cold anticyclone moved south from British Columbia and caused temperatures and dew points to plummet to record lows. Initiated by the intense anticyclone and cold air damming by the Coast and Cascade mountains, a strong pressure gradient formed rapidly behind the front, with the pressure gradient force oriented across the mountains.

Gap wind effects played an important role in the windstorm. A strong pressure ridge through Puget Sound during the storm was a direct

manifestation of gap wind effects and created a strong channel-parallel pressure gradient force. Thus the local winds were accelerated not only by the funneling through the channel, but also by the pressure gradient force as well. The gap winds were traced through Puget Sound using dew points and wind speed. Gap winds were the likely cause of the strong northerly winds and damage in Puget Sound.

The horizontal pressure gradient is the primary explanation used for other strong windstorms on the western slopes of the Cascade Mountains (Mass and Albright, 1985; Reed, 1981). However, as pointed out by Colman and Dierking, data from these storms indicate conditions favorable for mountain wave acceleration. Also, the horizontal pressure gradient does not explain the rapid onset of the destructive winds in the early morning hours on 28 December 1990. In addition, gap winds cannot explain the microburst-type damage on the San Juan Islands.

Mountain wave amplification was the probable mechanism for the extreme winds over San Juan Islands since the criteria for mountain wave amplification were present during the storm. Close examination of the vertical structure of the atmosphere upwind during the peak of the storm revealed a shallow inversion at ridge top, a critical layer (flow reversal) aloft and cross-mountain flow. These criteria have frequently been associated with previously studied downslope windstorms and are considered necessary for mountain wave amplification.

Tree fall on Guemes Island exhibited an interesting pattern of small, 200 m long swaths, similar in appearance to damage caused by traveling microbursts. The swaths occurred in groups that were oriented perpendicular to the mean wind. The size and orientation of the swaths were remarkably like the damage

pattern of another severe windstorm in the lee of the Cascades. Since evidence suggests that mountain wave amplification was likely occurring during the storm, these microbursts were most likely due to pulsations in the dynamically unstable downslope flow.

Transient pulsation in the severe downslope windstorm have been modeled numerically by Clark and Farley, (1984) Peltier and Scinocca, (1990) and more recently by Miranda and James (1992). Experiments reveal quasi-periodic oscillations in the downstream flow after the onset of the wave-breaking. These high velocity pulsations were imbedded within the low-level jet and extended well downstream of the mountain. These oscillations are likely the result of Kelvin-Helmholtz instability (Long, 1953, 1955; Peltier and Scinocca, 1990; Smith, 1991). It is proposed that the damage in the San Juan Islands was due to orographic microbursts in a lee-side mountain wave.

In summary, synoptic scale movement of an arctic anticyclone and the cold air damming east of the mountains of the Pacific Northwest, set up the strong pressure gradient. The combination of the movement of a mid-level short wave trough over the mountains, the cold air damming, and cross-mountain flow created the ideal mountain-wave amplification environment. Thus the severe winds observed during the pre-dawn hours were caused by orographic microbursts in the downslope flow.

Since gap winds occur frequently in Washington State, the forecast for an exceptionally strong windstorm is difficult. The problem forecast is complicated by the concurrent effects of mountain wave amplification. However, when the synoptic situation indicates a strong pressure gradient across the mountains and cross mountain flow in the lower levels, the forecaster should examine the upstream sounding for mountain-wave criteria.

The criteria are: a stable layer above the upstream ridge, cross-barrier flow at ridgetop and a mid-level critical layer. By distinguishing between gap wind events with and without mountain-wave amplification, the forecaster can discern between the more common gale force winds of the gap wind event and the destructive microburst type winds of the mountain-wave event.

For future research, other downslope windstorm damage should be examined for the patterns caused by orographic microbursts. If these patterns are somewhat universal, new insights can be gained concerning the nature of the dynamically unstable downslope flow. Ideally, other mesoscale observing techniques such as Doppler lidar, and high-time-resolution wind sensors should be employed during the storms in Washington.

Although these exceptional events are rare, a climatology of many storms over western Washington State is needed. The climatology would provide the typical synoptic scale and mesoscale environment of the local windstorms. This case study suggests that the necessary environment for local severe downslope windstorms requires not only cross-mountain flow and a stable layer at ridgetop, but also a mid-level short wave trough to act as the critical layer needed for vertical wave energy reflection. The climatology can also indicate the necessary height and strength of the stable layer, the specific strength and direction of the cross-mountain flow and the average height of the critical layer.

More knowledge of the mechanisms important to this storm can be gained through numerical experiments on a local mesoscale model. The relative importance of gap wind effects and mountain-wave amplification may be discerned. Also, by varying the upstream wind direction at ridge-top, the experiments would indicate regions of most severe winds downstream. These

experiments would aid in the prediction of local severe winter windstorms.

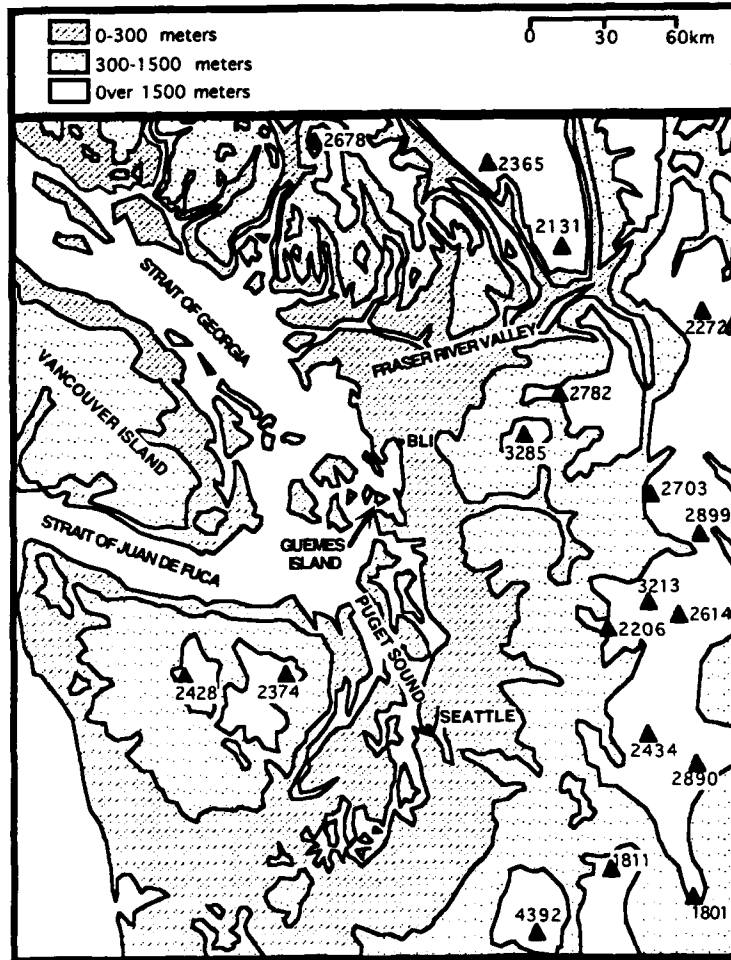


Figure 1. Location and topographic map of western Washington and southwest British Columbia. (after Overland and Walter, 1981).



Figure 2. One of the trees toppled by the storm. Photo courtesy of Ferdi Businger.

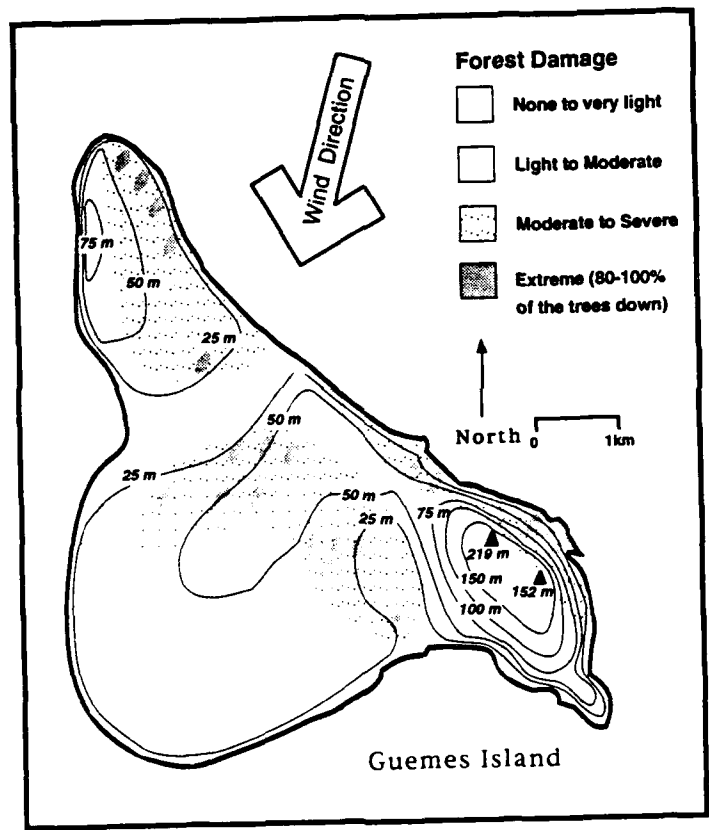


Figure 3. Forest damage on Guemes Island.

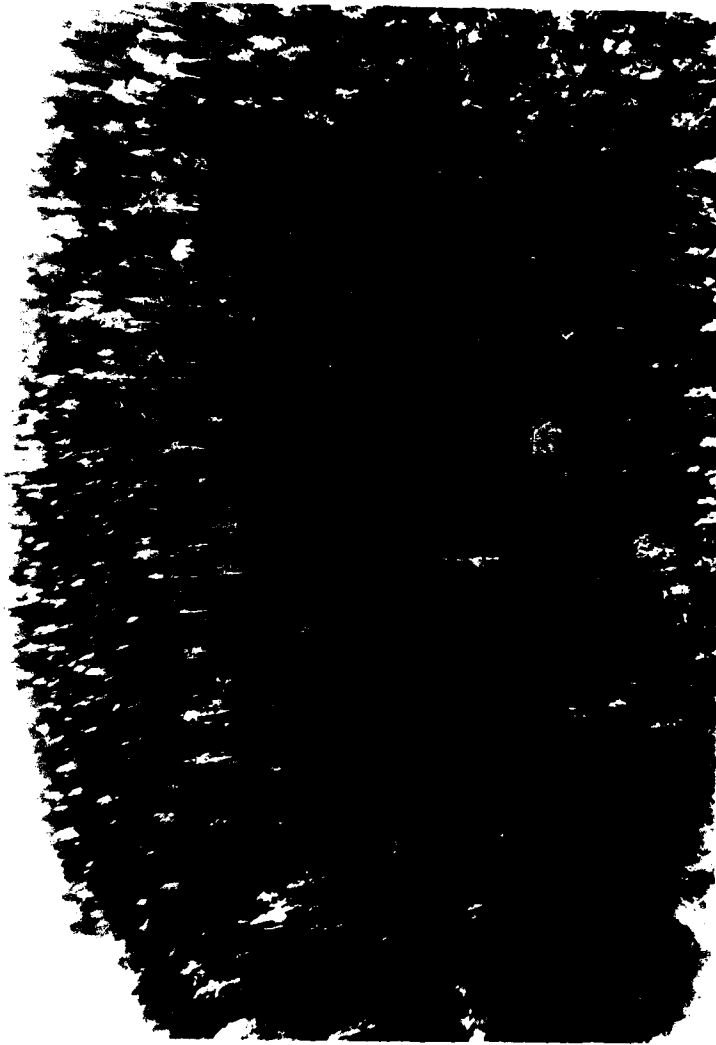


Figure 4. Aerial photo of damage swath. Photo courtesy of Win Anderson, Guemes Island, WA.

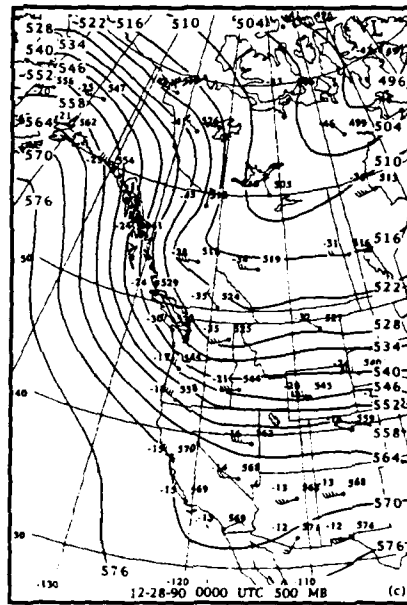
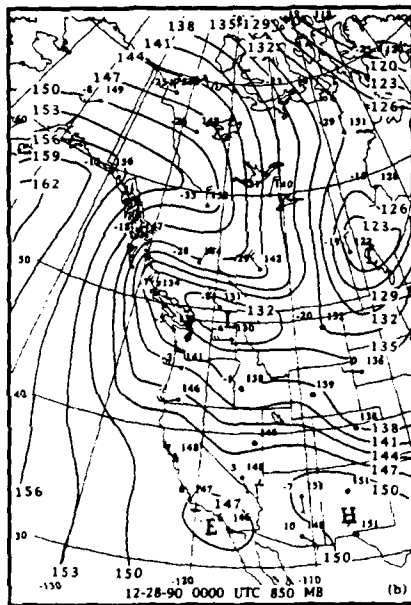
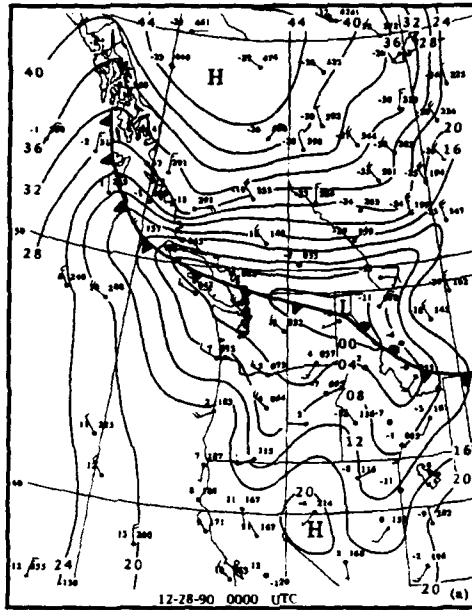


Figure 6. Same as figure 5 except for 0000 UTC 28 December 1990.

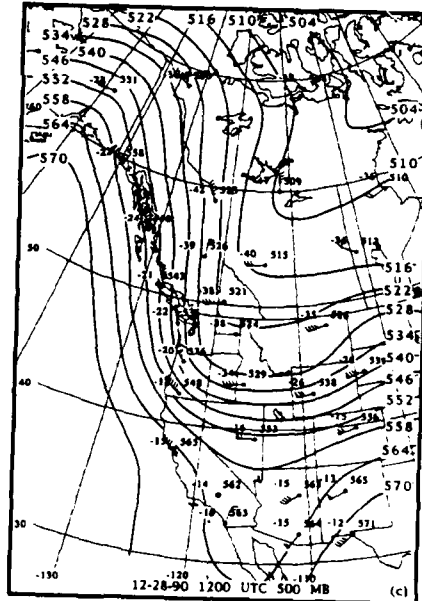
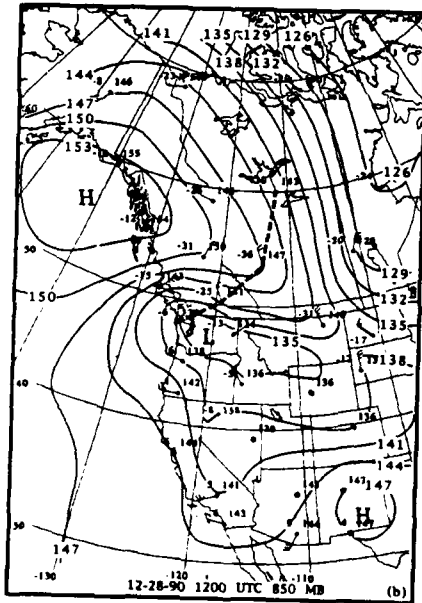
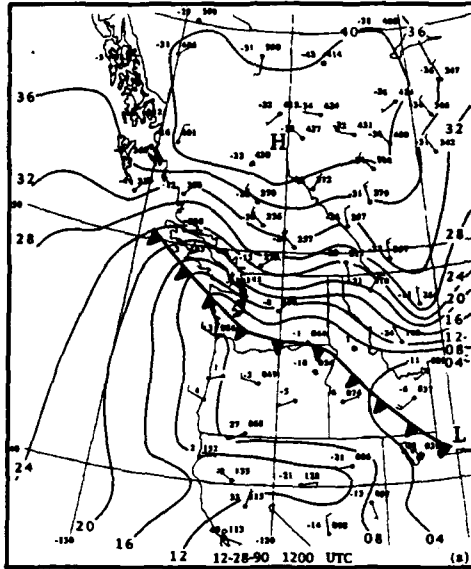


Figure 7. Same as figure 5 except for 1200 UTC 28 December 1990.

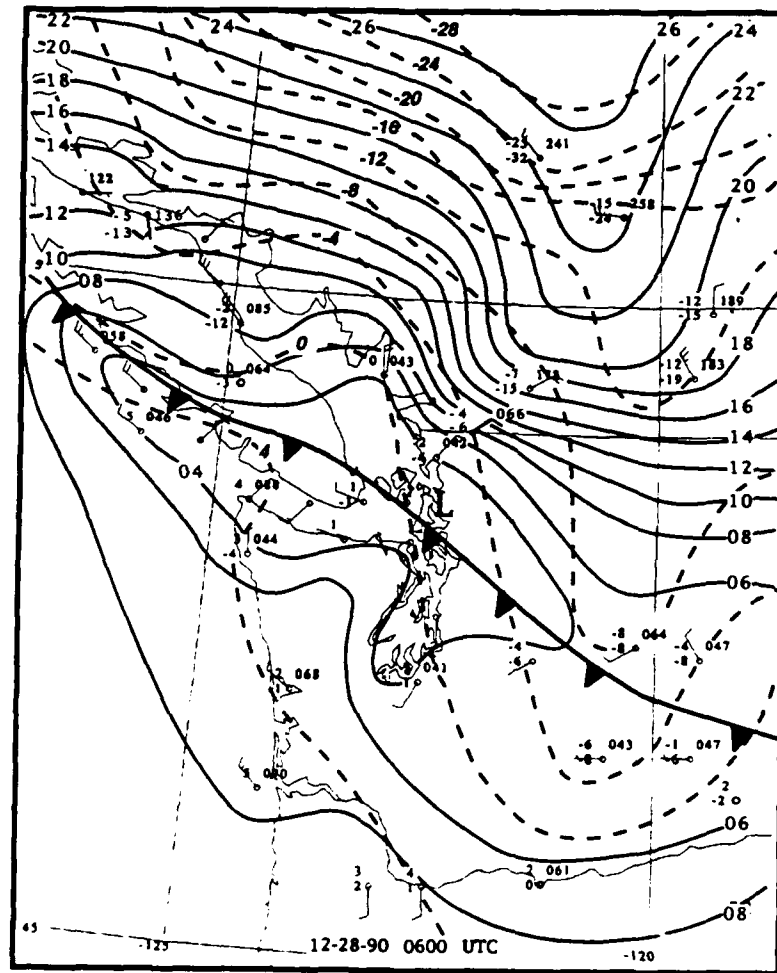


Figure 10. Regional surface chart for 0600 UTC 28 December 1990. Solid lines, sea level pressure at 2 mb intervals. Dashed lines, temperature at 4°C intervals. Station plots are same as surface charts in figure 5 except dew point is added below temperature plot.

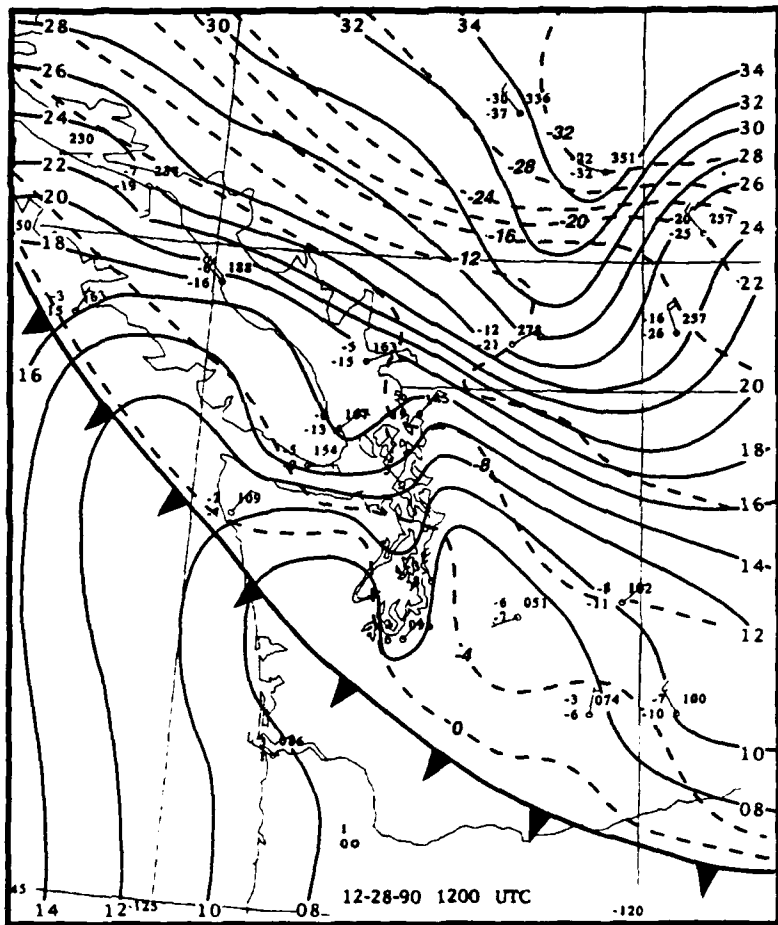


Figure 11. Regional surface chart for 1200 UTC 28 December 1990. Analysis same as figure 10.

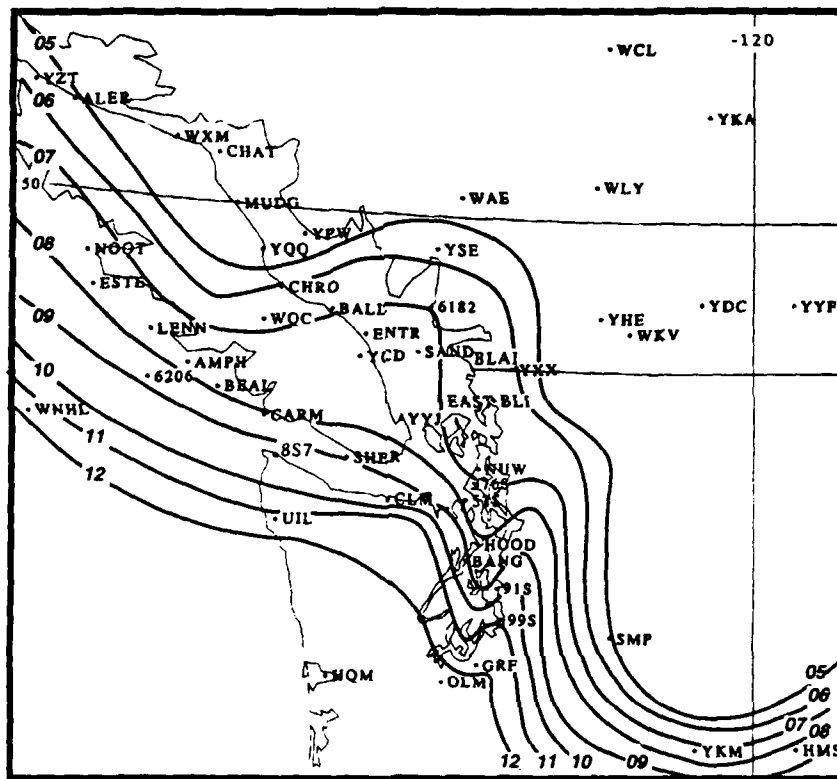


Figure 12. Time of arrival at selected stations of the arctic air mass based on dew point (4°C) and wind velocity (10 m s^{-1}). Arrival times begin at 0500 UTC 28 December 1990 to 1200 UTC 28 December 1990.

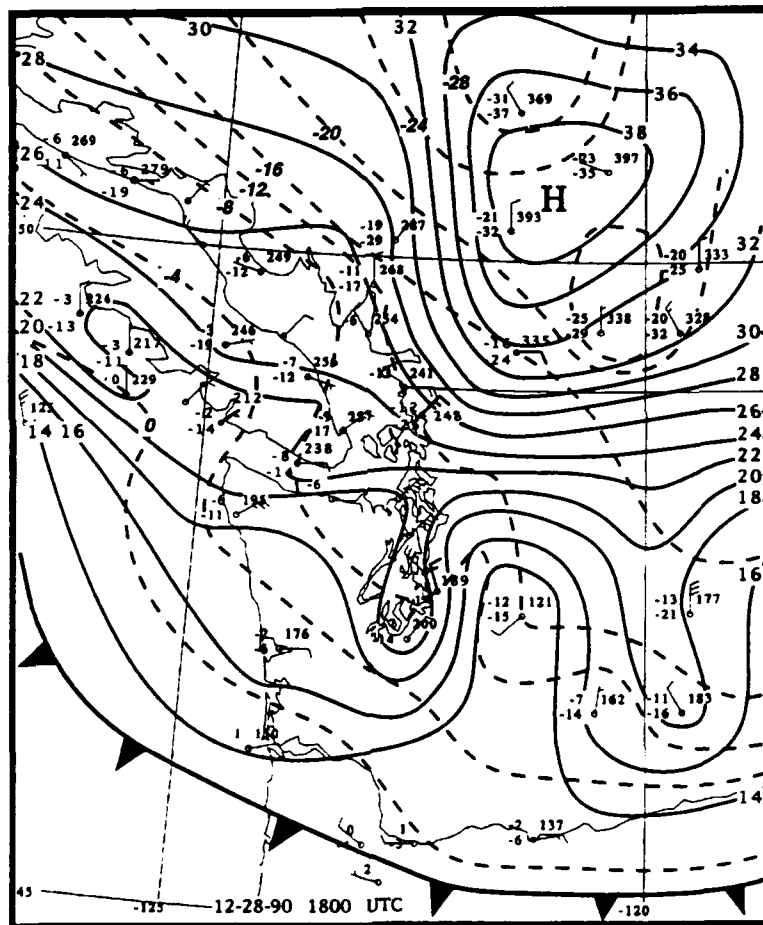


Figure 13. Regional surface chart for 1800 UTC 28 December 1990. Analysis same as figure 10.

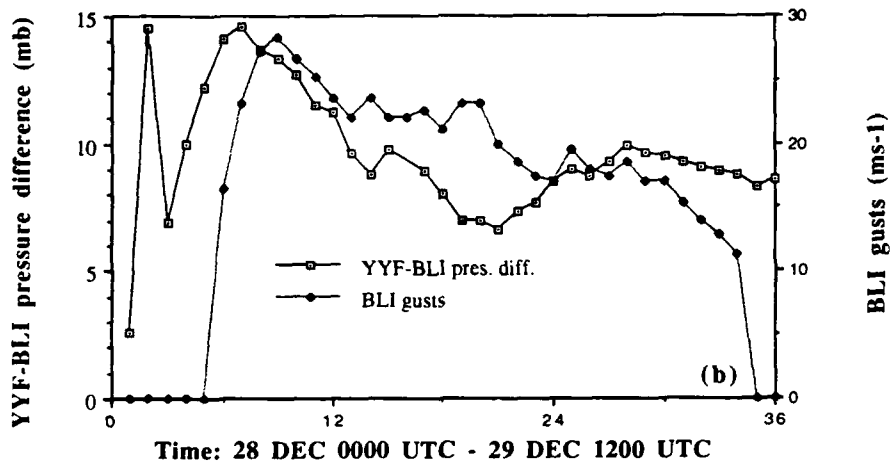
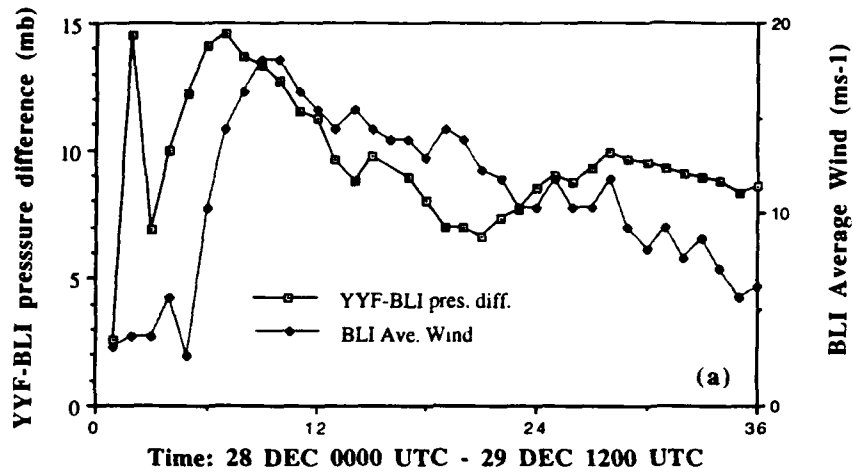


Figure 14. Comparison of pressure difference between BLI and YYF and average wind speed (a) and gust wind speeds (b) at BLI.

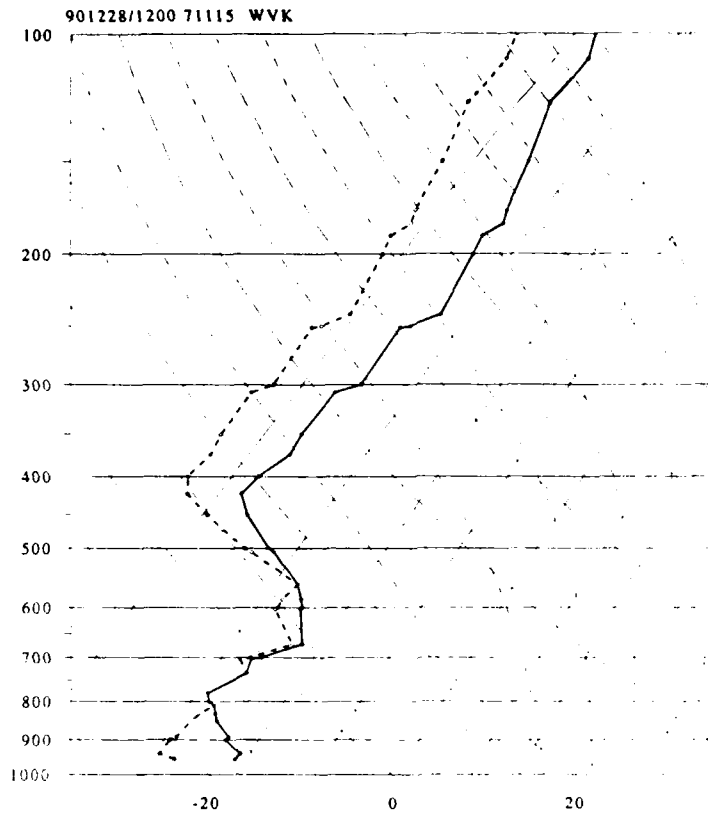


Figure 15. Skew T -log p plot: Temperature (heavy solid), dew point (heavy dashed) and wind vertical profile for Vernon, British Columbia at 1200 UTC 28 December 1990. Wind plots same as convention in figure 3. Isobars (mb) are straight horizontal lines. Dry adiabats are slightly curved dot dashed lines slanted from lower right to upper left. Saturated adiabats are curved short dashed lines sloped lower right to upper left. Saturation mixing ratio are dashed lower left to upper right lines.

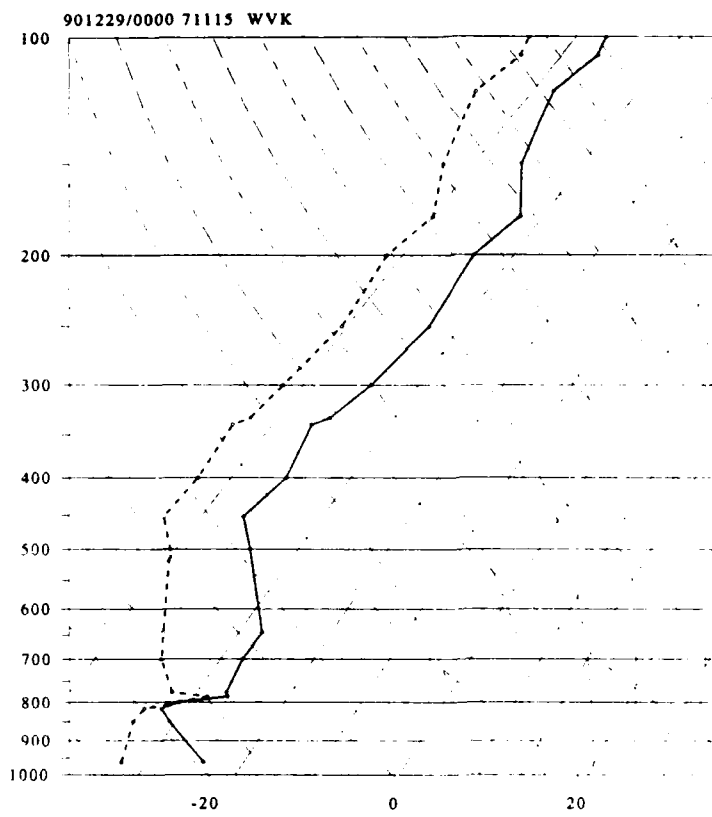


Figure 16. Same as figure 15 except for 0000 UTC 29 December 1990.

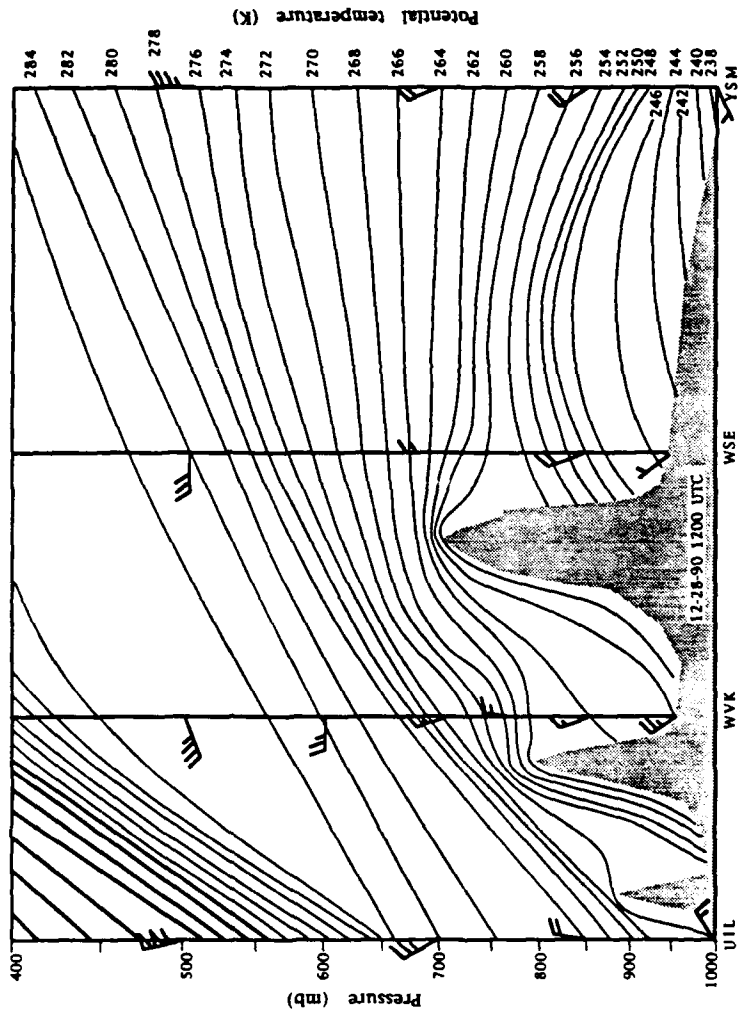


Figure 17. Cross section of potential temperature (K) along dashed line in figure 7(b). Wind plot convention is same as figure 5.

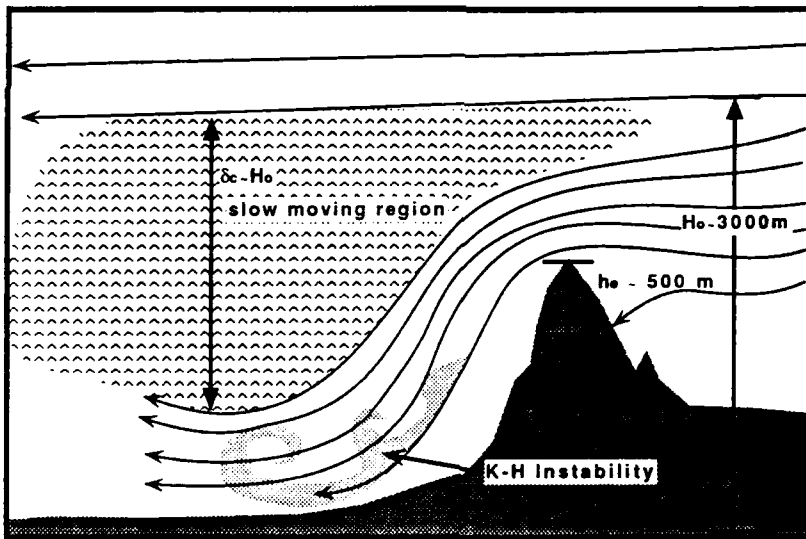


Figure 18. Idealized schematic of the downslope windstorm of 28 December 1990. For further explanation see text.

REFERENCES

- Bedard, A. J. Jr., 1990: A review of the evidence for strong, small-scale vortical flows during downslope windstorms. *J. of Wind Engineering and Industrial Aerodynamics*, **36**, 97-106.
- Bell, G.D. and L. F. Bosart, 1988: Appalachian cold-air damming. *Mon. Wea. Rev.* **116**, 137- 161.
- Bower, J. B. and D. R. Durran, 1986: A study of wind profiler data collected upstream during windstorms in Boulder, Colorado. *Mon. Wea. Rev.*, **114**, 1491-1500.
- Brinkmann, W. A. R., 1974: Strong downslope winds at Boulder, Colorado. *Mon. Wea. Rev.*, **102**, 592-602.
- Businger, S., W. H. Bauman and G.F. Watson, 1991: The development of the Piedmont Front and associated outbreak of severe weather on 13 March 1986. *Mon. Wea. Rev.* , **119**, 2224-2251.
- Clark, T. L. and R. D. Farley, 1984: Severe downslope windstorm calculations in two and three spatial dimensions using anelastic interactive grid nesting: A possible mechanism for gustiness. *J. Atmos. Sci.*, **41**, 329-350.
- Clark, T. L., and W. R. Peltier, 1977: On the evolution and stability of finite amplitude mountain waves. *J. Atmos. Sci.*, **34**, 1715-1730.
- _____, and _____, 1984: Critical level reflection and resonant growth of nonlinear mountain waves. *J. Atmos. Sci.*, **41**, 3122-3134.
- Colman, B. R. and C. F. Dierking, 1992: The Taku Wind of southeast Alaska: Its identification and prediction. *Wea. Forecasting*, **7**, 49-64.
- Dunn, L. , 1987: Cold-air damming by the Front Range of the Colorado Rockies and its relationship to locally heavy snows. *Wea. Forecasting*, **2**, 177-189.

- Durran, D.R., 1986: Another look at downslope windstorms. Part I: The development of analogs to supercritical flow in an infinitely deep, continuously stratified fluid. *J. Atmos. Sci.*, **43**, 2527-2543.
- _____, 1990: Mountain waves and downslope windstorms. *Atmospheric Processes over Complex Terrain*, W. Blumen, Ed., Amer. Meteor. Soc., 59-81.
- _____, and J. B. Klemp, 1982: The effects of moisture on trapped mountain lee waves. *J. Atmos. Sci.*, **39**, 2490-2506.
- Fujita, T. J., 1985: The Downburst. University of Chicago. 122 pp.
- Klemp, J. B. and D. K. Lilly, 1975: The dynamics of wave-induced downslope winds. *J. Atmos. Sci.*, **32**, 320-339.
- Lilly D. K. and J. B. Klemp, 1979: The effects of terrain shape on nonlinear hydrostatic mountain waves. *J. Fluid Mech.*, **95**, 241-261.
- Long, R. R., 1953: Some Aspects of stratified Fluids, I. A theoretical investigation. *Tellus*, **5**, 42-58.
- _____, 1955: Some aspects of stratified fluids III. Continuous density gradients. *Tellus*, **1**, 341-357.
- Mass, C.A. and M. D. Albright, 1985: A severe windstorm in the lee of the Cascade Mountains of Washington State. *Mon. Wea. Rev.*, **113**, 1261-1281.
- Miranda, P. M. A., and I. N. James, 1992: Non-linear three-dimensional effects on gravity-wave drag: Splitting flow and breaking waves. *Quart. J. Roy. Meteor. Soc.*, **118**, 1057-1081.
- National Oceanic and Atmospheric Administration, U.S. Department of Commerce. *Storm Data*. (Available from National Climatic Data Center, Asheville, NC 28801).
- Nieman, P. J., R. M. Hardesty, M. A. Shapiro, and R. E. Cupp, 1988: Doppler lidar observations of a downslope windstorm. *Mon. Wea. Rev.*, **116**, 2265-2275.

- Overland, J. E. and B. A. Walter, 1981: Gap winds in the Strait of Juan de Fuca. *Mon. Wea. Rev.*, **109**, 2221-2233.
- Peltier, W. R., and T. L. Clark, 1979: The evolution and stability of finite-amplitude mountain waves. Part II: Surface wave drag and severe downslope windstorms. *J. Atmos. Sci.*, **36**, 1498-1529.
- _____, and _____, 1983: Nonlinear mountain waves in two and three spatial dimensions. *Quart. J. Roy. Meteor. Soc.*, **109**, 527-548.
- _____ and J. F. Scinocca, 1990: The origin of severe downslope windstorm Pulsations. *J. Atmos. Sci.*, **47**, 2853-2870.
- Reed, R. J., 1981: A case study of a Bora-like windstorm in western Washington. *Mon. Wea. Rev.*, **109**, 2383-2393.
- Reed, T. R., 1931: Gap winds of the Strait of Juan de Fuca. *Mon. Wea. Rev.*, **59**, 373-376.
- Richwein, B. A., 1980: The damming effect of the southern Appalachians. *Natl. Wea. Dig.*, **5**, 2-12.
- Scorer, R. S., 1949: Theory of waves in the lee of mountains. *Quart. J. Meteor. Soc.*, **75**, 41-56.
- Smith, R. B., 1985: On severe downslope winds. *J. Atmos. Sci.*, **42**, 2597-2603.
- _____, 1987: Aerial observations of the Yugoslavian Bora. *J. Atmos. Sci.*, **44**, 269-297.
- _____, and J. Sun, 1987: Generalized hydraulic solutions pertaining to severe downslope winds. *J. Atmos. Sci.*, **44**, 2934-2939.
- _____, 1991: Kelvin-Helmholtz instability in severe downslope wind flow. *J. Atmos. Sci.*, **48**, 1319-1324.